Effective Medium Model for Multilayered Anisotropic Media with Different Orientations

Yang Bao and Jiming Song

Department of Electrical and Computer Engineering
Iowa State University, Ames, 50011, Iowa
brianbao@iastate.edu, jisong@iastate.edu

Abstract **─** An efficient model is developed to simulate multilayered biaxial anisotropic material with different orientations by using effective medium theory. Equivalent model is used to extract effective permittivity, permeability and orientation angle for multilayered biaxial anisotropic medium. Analytical expressions for effective parameters and orientation angle are derived for low frequency (LF) limit. The model also gives a non-magnetic effective anisotropic layer if each layer is non-magnetic anisotropic dielectric. Good agreement is achieved by comparing the effective parameters extracted with and without low frequency approximation. We show that the frequency-independent equivalent model is valid for frequency up to 10 GHz.

Index Terms **─** Effective medium theory, multilayered anisotropic media, parameter extraction.

I. INTRODUCTION

Anisotropic property is very popular among modern engineering materials such as composites, fibers, crystals, wood and so on. These kinds of materials have a lot of usages as housings and casings in aerospace, transportation, civil infrastructure, electronics, appliance and marine due to its characteristics such as: low weight, less tooling costs, high stiffness, low corrosion and easy to fabricate [1-5]. In aerospace industry, composites can be replacements for metals due to its good features that they are not as electrically conductive as traditional ones [2]. Thus, it becomes more and more important to understand the electromagnetic interactions (i.e., reflection, transmission) of composites [3, 5]. Multilayered anisotropic material with different orientations is very common in composites. However, electromagnetic modelling of multilayered anisotropic material needs huge CPU time and memory requirements. Using effective medium theory, by combining multilayered anisotropic medium with a single equivalent layer for the permittivity, permeability and orientation, CPU time and memory requirements can be significantly reduced [6].

In this paper, effective medium theory is applied to model multilayered biaxial anisotropic material with different orientations for a plane wave incidence at the normal direction. Basing on the same reflection and transmission coefficients, effective permittivity, permeability and orientation angle are extracted, similar to the approach used to extract effective parameters from measurements and numerical modeling of periodic structures as isotropic materials. With the low frequency (LF) limit, analytical expressions for effective parameters and orientation angle are derived and result in a frequency-independent equivalent model. Finally, effective parameters using low frequency approximation are compared with the ones from parameter extraction method. Good agreements in effective parameters and angle are observed between with and without the approximations for the frequency up to 10 GHz.

II. FORMULATION

In Fig. 1, the equivalent model is presented for multilayered biaxial anisotropic media with different orientations between two half spaces. A plane wave travels at the normal direction (z direction) to x-y plane. A global Cartesian coordinate x-y-z is used in the two half spaces and local coordinate x'-y'-z for each layer between two half spaces with x'_n rotating θ_n from x. The relative permeability and permittivity of the biaxial anisotropic layer can be expressed in tensor form as $\bar{\boldsymbol{\mu}}_n = \mathrm{diag}(\mu_{xn}, \mu_{yn}, \mu_{zn})$, $\bar{\boldsymbol{\varepsilon}}_n = \mathrm{diag}(\varepsilon_{xn}, \varepsilon_{yn}, \varepsilon_{zn})$.

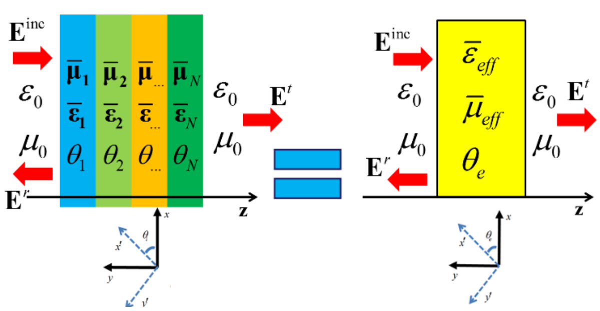

Fig. 1. Multilayered biaxial anisotropic media and its equivalent single layer model.

Submitted On: November 17, 2016
Accepted On: February 14, 2017

A. Reflection and transmission coefficient for equivalent layer

For the equivalent layer model, suppose electromagnetic field propagates in z direction with electric field polarized in x and y directions. We can get reflection and transmission coefficient matrices by expressing the electromagnetic field in all three regions and matching boundary conditions. The reflection coefficient **R** and transmission coefficient **T** are 2 by 2 matrices and are defined similar to S parameters [7]:

$$\begin{aligned} R_{pp} &= A_p \cos^2\theta_e + A_{\tilde{p}} \sin^2\theta_e, \\ R_{yx} &= R_{xy} = \left(A_x - A_y\right)\sin\theta_e \cos\theta_e, \\ T_{pp} &= B_p \cos^2\theta_e + B_{\tilde{p}} \sin^2\theta_e, \\ T_{yx} &= T_{xy} = \left(B_x - B_y\right)\sin\theta_e \cos\theta_e, \end{aligned} \quad (1)$$

where

$$A_p = \frac{\Gamma_{0p}\left(1-e^{-2j\beta_p d_t}\right)}{1-\Gamma_{0p}^2 e^{-2j\beta_p d_t}}, \quad B_p = \frac{\left(1-\Gamma_{0p}^2\right)e^{-jd_t\beta_p}}{1-\Gamma_{0p}^2 e^{-2j\beta_p d_t}}, \quad \Gamma_{0p} = \frac{\tilde{\eta}_p - 1}{\tilde{\eta}_p + 1},$$

$$\beta_p = \beta_0\sqrt{\varepsilon_{pe}\mu_{\tilde{p}e}}, \quad \tilde{\eta}_p = \sqrt{\frac{\mu_{\tilde{p}e}}{\varepsilon_{pe}}}, \quad p = x, y, \quad \tilde{p} = \begin{cases} x, & p = y \\ y, & p = x \end{cases}.$$

A_p and B_p are the same as the reflection and transmission coefficients derived using isotropic layer with $\mu_{\tilde{p}}$ and ε_p. d_t is the total thickness and $\beta_0 = \omega\sqrt{\varepsilon_0\mu_0}$.

B. Reflection and transmission coefficients for multilayers

The first method to derive the reflection and transmission matrices is similar to the transmission line theory. For region n (1 to N), $z_n < z < z_{n+1}$, z there are two types of propagation modes in local coordinate:

$$\mathbf{E}_n = \begin{bmatrix} E_{nx'} \\ E_{ny'} \end{bmatrix} = \left[e^{-j\bar{\boldsymbol{\beta}}_n(z-z_{n+1})} + e^{j\bar{\boldsymbol{\beta}}_n(z-z_{n+1})}\bar{\mathbf{R}}^-_{n,n+1} \right] \begin{bmatrix} A_n \\ B_n \end{bmatrix}, \quad (2)$$

$$\begin{aligned} \eta_0 \bar{\mathbf{Z}}_{n0} \bullet \mathbf{H}_n &= \eta_0 \begin{bmatrix} \eta_{nx} & 0 \\ 0 & \eta_{ny} \end{bmatrix} \begin{bmatrix} H_{ny'} \\ -H_{nx'} \end{bmatrix} \\ &= \left[e^{-j\bar{\boldsymbol{\beta}}_n(z-z_{n+1})} - e^{j\bar{\boldsymbol{\beta}}_n(z-z_{n+1})}\bar{\mathbf{R}}^-_{n,n+1} \right] \begin{bmatrix} A_n \\ B_n \end{bmatrix}, \end{aligned} \quad (3)$$

where $\bar{\mathbf{Z}}_{n0} = \mathrm{diag}\left(\eta_{nx}, \eta_{ny}\right)$, $\bar{\boldsymbol{\beta}}_n = \mathrm{diag}\left(\beta_{nx}, \beta_{ny}\right)$, $\bar{\mathbf{R}}^-_{n,n+1}$ is the 2 by 2 reflection matrix in region n at z_{n+1}.

The fields also can be written in the global coordinate

$$\begin{bmatrix} E_{nx'} \\ E_{ny'} \end{bmatrix} = \bar{\mathbf{O}}_n \begin{bmatrix} E_{nx} \\ E_{ny} \end{bmatrix}, \quad \begin{bmatrix} H_{ny'} \\ -H_{nx'} \end{bmatrix} = \bar{\mathbf{O}}_n \begin{bmatrix} H_{ny} \\ -H_{nx} \end{bmatrix}, \quad (4)$$

where the rotation matrix $\bar{\mathbf{O}}_n$ is given as:

$$\bar{\mathbf{O}}_n = \begin{bmatrix} \cos\theta_n & \sin\theta_n \\ -\sin\theta_n & \cos\theta_n \end{bmatrix}, \quad \bar{\mathbf{O}}_n^{-1} = \bar{\mathbf{O}}_n^T. \quad (5)$$

The relation between the electric and magnetic fields at $z = z_{n+1}$ is:

$$\mathbf{E}_n(z_{n+1}) = \eta_0 \bar{\mathbf{Z}}^-_{n,n+1} \bullet \mathbf{H}_n(z_{n+1}), \quad (6)$$

$\bar{\mathbf{Z}}^-_{n,n+1}$ is the input impedance at $z = z_{n+1}$. Submitting (2) and (3) into (6) yields:

$$\bar{\mathbf{R}}^-_{n,n+1} = \left[\bar{\mathbf{Z}}^-_{n,n+1}\bar{\mathbf{Z}}^{-1}_{n0} + \bar{\mathbf{I}}\right]^{-1}\left[\bar{\mathbf{Z}}^-_{n,n+1}\bar{\mathbf{Z}}^{-1}_{n0} - \bar{\mathbf{I}}\right], \quad (7)$$

where $\bar{\mathbf{I}} = \mathrm{diag}(1,1)$ and matrix multiplications are involved. At $z = z_n$, similarly, we have:

$$\mathbf{E}_n(z_n) = \eta_0 \bar{\mathbf{Z}}^+_{n-1,n} \bullet \mathbf{H}_n(z_n). \quad (8)$$

It is found that,

$$\begin{aligned} \bar{\mathbf{Z}}^+_{n-1,n} &= \left[\bar{\mathbf{I}} + e^{-j\bar{\boldsymbol{\beta}}_n d_n}\bar{\mathbf{R}}^-_{n,n+1}e^{-j\bar{\boldsymbol{\beta}}_n d_n}\right] \\ &\quad \cdot \left[\bar{\mathbf{I}} - e^{-j\bar{\boldsymbol{\beta}}_n d_n}\bar{\mathbf{R}}^-_{n,n+1}e^{-j\bar{\boldsymbol{\beta}}_n d_n}\right]^{-1}\bar{\mathbf{Z}}_{n0}, \end{aligned} \quad (9)$$

where $d_n = z_{n+1} - z_n$. At the interface, the tangential components of both electric and magnetic fields should be continuous. Using the equations above, we find the impedance matrices at two sides and field components as:

$$\bar{\mathbf{Z}}^-_{n-1,n} = \bar{\mathbf{O}}_{n-1}\bar{\mathbf{O}}_n^T\bar{\mathbf{Z}}^+_{n-1,n}\bar{\mathbf{O}}_n\bar{\mathbf{O}}_{n-1}^T, \quad (10)$$

$$\begin{aligned} \begin{bmatrix} A_n \\ B_n \end{bmatrix} &= e^{-j\bar{\boldsymbol{\beta}}_n d_n}\left[\bar{\mathbf{I}} + e^{-j\bar{\boldsymbol{\beta}}_n d_n}\bar{\mathbf{R}}^-_{n,n+1}e^{-j\bar{\boldsymbol{\beta}}_n d_n}\right]^{-1} \\ &\quad \cdot \bar{\mathbf{O}}_n\bar{\mathbf{O}}_{n-1}^T\left[\bar{\mathbf{I}} + \bar{\mathbf{R}}^-_{n-1,n}\right]\begin{bmatrix} A_{n-1} \\ B_{n-1} \end{bmatrix}. \end{aligned} \quad (11)$$

In Region 0, which is the half-space for the incident wave, the electric field is written as:

$$\mathbf{E}_0 = \begin{bmatrix} E_{0x} \\ E_{0y} \end{bmatrix} = \left[e^{-j\bar{\boldsymbol{\beta}}_0(z-z_1)} + e^{-j\bar{\boldsymbol{\beta}}_0(z-z_1)}\bar{\mathbf{R}}\right]\begin{bmatrix} A_0 \\ B_0 \end{bmatrix}, \quad (12)$$

where $\bar{\mathbf{R}} = \bar{\mathbf{R}}^-_{0,1}$ is the reflection matrix defined at $z = z_1$ and can be calculated recursively using (10), (7) and (9) with $\bar{\mathbf{Z}}^+_{N,N+1} = \bar{\mathbf{Z}}_{(N+1)0} = \bar{\mathbf{I}}$.

In the half-space Region $N+1$, the electric field is written as:

$$\mathbf{E}_{N+1} = \begin{bmatrix} E_{N+1\,x} \\ E_{N+1\,y} \end{bmatrix} = e^{-j\bar{\boldsymbol{\beta}}_0(z-z_{N+1})}\,\bar{\mathbf{T}}\begin{bmatrix} A_0 \\ B_0 \end{bmatrix}. \quad (13)$$

Using (11) recursively, the total transmission matrix defined at $z = z_{N+1}$ is represented as:

$$\begin{aligned} \bar{\mathbf{T}} &= \bar{\mathbf{O}}_N^T\left[\bar{\mathbf{I}} + \bar{\mathbf{R}}^-_{N,N+1}\right] \\ &\cdot \prod_{n=1}^{N} e^{-j\bar{\boldsymbol{\beta}}_n d_n}\left[\bar{\mathbf{I}} + e^{-j\bar{\boldsymbol{\beta}}_n d_n}\bar{\mathbf{R}}^-_{n,n+1}e^{-j\bar{\boldsymbol{\beta}}_n d_n}\right]^{-1}\bar{\mathbf{O}}_n\bar{\mathbf{O}}_{n-1}^T\left[\bar{\mathbf{I}} + \bar{\mathbf{R}}^-_{n-1,n}\right], \end{aligned} \quad (14)$$

where $d_{N+1} = 0$, $\bar{\mathbf{O}}_0 = \bar{\mathbf{O}}_{N+1} = \bar{\mathbf{I}}$.

Another method to get total reflection and transmission coefficients for multilayers can be followed an approach in [8]. The basic idea is to calculate reflection and transmission coefficients from an interface between two half spaces and then get total reflection and transmission coefficients recursively.

When Regions n and $n+1$ are half-space, the electric and magnetic fields at the interface are written in local coordinates as:

$$\mathbf{E}_n = \begin{bmatrix} E_{nx'} \\ E_{ny'} \end{bmatrix} = \left[\bar{\mathbf{I}} + \bar{\mathbf{R}}_{n,n+1}\right] e^{-j\bar{\boldsymbol{\beta}}_n d_n} \begin{bmatrix} A_n \\ B_n \end{bmatrix}, \quad \eta_0 \bar{\mathbf{Z}}_{n0} \bullet \mathbf{H}_n = \left[\bar{\mathbf{I}} - \bar{\mathbf{R}}_{n,n+1}\right] e^{-j\bar{\boldsymbol{\beta}}_n d_n} \begin{bmatrix} A_n \\ B_n \end{bmatrix}, \tag{15}$$

$$\mathbf{E}_{n+1} = \begin{bmatrix} E_{(n+1)x'} \\ E_{(n+1)y'} \end{bmatrix} = \bar{\mathbf{T}}_{n,n+1} e^{-j\bar{\boldsymbol{\beta}}_n d_n} \begin{bmatrix} A_n \\ B_n \end{bmatrix}, \quad \eta_0 \bar{\mathbf{Z}}_{(n+1)0} \bullet \mathbf{H}_{(n+1)} = \bar{\mathbf{T}}_{n,n+1} e^{-j\bar{\boldsymbol{\beta}}_n d_n} \begin{bmatrix} A_n \\ B_n \end{bmatrix}. \tag{16}$$

Matching the boundary conditions at the interface using the global coordinate yields:

$$\bar{\mathbf{O}}_n^T \left[\bar{\mathbf{I}} + \bar{\mathbf{R}}_{n,n+1}\right] = \bar{\mathbf{O}}_{n+1}^T \bar{\mathbf{T}}_{n,n+1}, \tag{17}$$

$$\bar{\mathbf{O}}_n^T \bar{\mathbf{Z}}_{n0}^{-1} \left[\bar{\mathbf{I}} - \bar{\mathbf{R}}_{n,n+1}\right] = \bar{\mathbf{O}}_{n+1}^T \bar{\mathbf{Z}}_{(n+1)0}^{-1} \bar{\mathbf{T}}_{n,n+1}. \tag{18}$$

The half-space reflection and transmission coefficients are found as:

$$\bar{\mathbf{R}}_{n,n+1} = \left[\bar{\mathbf{Z}}_{n0}^{-1} + \bar{\mathbf{O}}_n \bar{\mathbf{O}}_{n+1}^T \bar{\mathbf{Z}}_{(n+1)0}^{-1} \bar{\mathbf{O}}_{n+1} \bar{\mathbf{O}}_n^T\right]^{-1} \cdot \left[\bar{\mathbf{Z}}_{n0}^{-1} - \bar{\mathbf{O}}_n \bar{\mathbf{O}}_{n+1}^T \bar{\mathbf{Z}}_{(n+1)0}^{-1} \bar{\mathbf{O}}_{n+1} \bar{\mathbf{O}}_n^T\right], \tag{19}$$

$$\bar{\mathbf{T}}_{n,n+1} = \bar{\mathbf{O}}_{n+1} \bar{\mathbf{O}}_n^T \left[\bar{\mathbf{I}} + \bar{\mathbf{R}}_{n,n+1}\right] = 2\bar{\mathbf{O}}_{n+1} \bar{\mathbf{O}}_n^T \left[\bar{\mathbf{Z}}_{n0}^{-1} + \bar{\mathbf{O}}_n \bar{\mathbf{O}}_{n+1}^T \bar{\mathbf{Z}}_{(n+1)0}^{-1} \bar{\mathbf{O}}_{n+1} \bar{\mathbf{O}}_n^T\right]^{-1} \bar{\mathbf{Z}}_{n0}^{-1}. \tag{20}$$

It can be verified that the reflection matrix is symmetrical, but the transmission matrix is not in general, and,

$$\bar{\mathbf{R}}_{n+1,n} = -\bar{\mathbf{O}}_{n+1} \bar{\mathbf{O}}_n^T \bar{\mathbf{R}}_{n,n+1} \bar{\mathbf{O}}_n \bar{\mathbf{O}}_{n+1}^T, \tag{21}$$

$$\bar{\mathbf{T}}_{n+1,n} = \bar{\mathbf{O}}_n \bar{\mathbf{O}}_{n+1}^T \left[\bar{\mathbf{I}} + \bar{\mathbf{R}}_{n+1,n}\right] = \left[\bar{\mathbf{I}} - \bar{\mathbf{R}}_{n,n+1}\right] \bar{\mathbf{O}}_n \bar{\mathbf{O}}_{n+1}^T. \tag{22}$$

The total reflection and transmission coefficients in [8] can be written as:

$$\bar{\mathbf{R}}_{n,n+1}^{-} = \bar{\mathbf{R}}_{n,n+1} + \bar{\mathbf{T}}_{n+1,n} e^{-j\bar{\boldsymbol{\beta}}_{n+1} d_{n+1}} \bar{\mathbf{R}}_{n+1,n+2}^{-} \cdot \left[\bar{\mathbf{I}} - e^{-j\bar{\boldsymbol{\beta}}_{n+1} d_{n+1}} \bar{\mathbf{R}}_{n+1,n} e^{-j\bar{\boldsymbol{\beta}}_{n+1} d_{n+1}} \bar{\mathbf{R}}_{n+1,n+2}^{-}\right]^{-1} e^{-j\bar{\boldsymbol{\beta}}_{n+1} d_{n+1}} \bar{\mathbf{T}}_{n,n+1}, \tag{23}$$

$$\bar{\mathbf{T}} = \bar{\mathbf{T}}_{N,N+1} \prod_{n=1}^{N} \left[\bar{\mathbf{I}} - e^{-j\bar{\boldsymbol{\beta}}_n d_n} \bar{\mathbf{R}}_{n,n-1} e^{-j\bar{\boldsymbol{\beta}}_n d_n} \bar{\mathbf{R}}_{n,n+1}^{-}\right]^{-1} e^{-j\bar{\boldsymbol{\beta}}_n d_n} \bar{\mathbf{T}}_{n-1,n}. \tag{24}$$

C. Equivalent model and low frequency approximation

Basing on same reflection and transmission coefficients for the single equivalent layer and multilayer, we express θ_e, A_p and B_p as functions of the reflection and transmission coefficients of multilayer structures:

$$\tan 2\theta_{er} = \frac{2R_{xy}}{R_{xx} - R_{yy}}, \quad \tan 2\theta_{et} = \frac{2\bar{T}_{xy}}{T_{xx} - T_{yy}}, \tag{25}$$

$$A_{x,y} = \frac{1}{2}\left(R_{xx} + R_{yy}\right) \pm \frac{R_{xy}}{\sin 2\theta_{er}}, \quad B_{x,y} = \frac{1}{2}\left(T_{xx} + T_{yy}\right) \pm \frac{\bar{T}_{xy}}{\sin 2\theta_{et}}, \tag{26}$$

where $R_{xy} = R_{yx}, T_{xy} \neq T_{yx}, \bar{T}_{xy} = \frac{1}{2}\left(T_{xy} + T_{yx}\right)$, the " ± " is for *x*- and *y*-component, respectively.

Then the effective parameters of the effective medium can be calculated from A_p and B_p using the approach for the isotropic layer [9-13]. The flowchart summarizing this procedure is shown in Fig. 2.

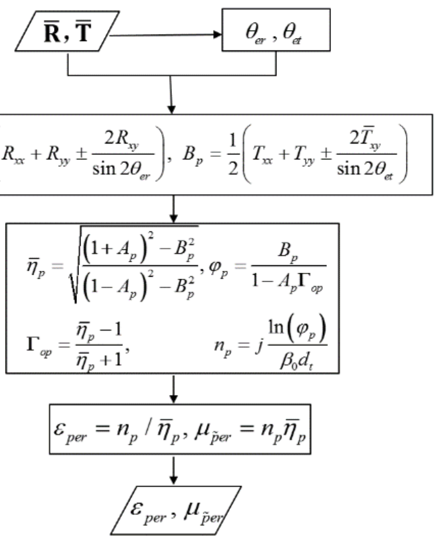

Fig. 2. Flowchart for effective parameters extraction.

For the low frequency limit, we follow the similar procedure to the isotropic case in [6]. The condition for low frequency approximation is satisfied when the wavelength is much bigger than the thickness of the structures. When $\beta_{np} d_n \ll 1$, applying Taylor series expansion to (9) and (14) and taking the first-order approximation yields:

$$e^{-j\bar{\boldsymbol{\beta}}_n d_n} \approx \bar{\mathbf{I}} - jd_n \bar{\boldsymbol{\beta}}_n. \tag{27}$$

Using $\bar{\mathbf{Z}}_{N,N+1}^{+} = \bar{\mathbf{Z}}_{(N+1)0} = \bar{\mathbf{I}}$, we have:

$$\bar{\mathbf{Z}}_{N,N+1}^{-} = \bar{\mathbf{O}}_N \bar{\mathbf{O}}_{N+1}^T \bar{\mathbf{Z}}_{N,N+1}^{+} \bar{\mathbf{O}}_{N+1} \bar{\mathbf{O}}_N^T = \bar{\mathbf{I}}, \tag{28}$$

$$\bar{\mathbf{R}}_{N,N+1}^{-} = \left[\bar{\mathbf{Z}}_{N,N+1}^{-} \bar{\mathbf{Z}}_{N0}^{-1} + \bar{\mathbf{I}}\right]^{-1} \left[\bar{\mathbf{Z}}_{N,N+1}^{-} \bar{\mathbf{Z}}_{N0}^{-1} - \bar{\mathbf{I}}\right] = \bar{\mathbf{\Gamma}}_N, \tag{29}$$

where $\bar{\mathbf{\Gamma}}_n = \mathrm{diag}\left(\mathbf{\Gamma}_{nx}, \mathbf{\Gamma}_{ny}\right)$. Since $\bar{\mathbf{\Gamma}}_n$ is a diagonal matrix, submitting it into (9) and using (27) yields:

$$\bar{\mathbf{Z}}^{+}_{N-1,N} = \bar{\mathbf{I}} + \bar{\mathbf{z}}^{+}_{N-1,N}, \quad \bar{\mathbf{z}}^{+}_{N-1,N} = j\beta_0 d_N \bar{\mathbf{\Delta}}_N, \tag{30}$$

where $\bar{\mathbf{\Delta}}_n = \mathrm{diag}\left(\mu_{ny} - \varepsilon_{nx}, \mu_{nx} - \varepsilon_{ny}\right)$. In deriving (30) we use the relations $\bar{\mathbf{D}}_1\bar{\mathbf{D}}_2 = \bar{\mathbf{D}}_2\bar{\mathbf{D}}_1$, if both $\bar{\mathbf{D}}_1$ and $\bar{\mathbf{D}}_2$ are diagonal, and $\left[\bar{\mathbf{A}} + \bar{\mathbf{B}}\right]^{-1} \approx \bar{\mathbf{A}}^{-1} - \bar{\mathbf{A}}^{-1}\bar{\mathbf{B}}\bar{\mathbf{A}}^{-1}$, if $\left\|\bar{\mathbf{A}}\right\| \gg \left\|\bar{\mathbf{B}}\right\|$. Using (10) and (28), we have,

$$\bar{\mathbf{Z}}^{-}_{N-1,N} = \bar{\mathbf{I}} + \bar{\mathbf{z}}^{-}_{N-1,N}, \tag{31}$$

where $\bar{\mathbf{z}}^{-}_{N-1,N} = j\beta_0 d_N \bar{\mathbf{O}}_{N-1}\bar{\mathbf{O}}^T_N \bar{\mathbf{\Delta}}_N \bar{\mathbf{O}}_N \bar{\mathbf{O}}^T_{N-1}$.

Submitting (31) into (7) yields:

$$\bar{\mathbf{R}}^{-}_{N-1,N} \approx \bar{\mathbf{\Gamma}}_{N-1} + \left[\bar{\mathbf{Z}}^{-1}_{(N-1)0} + \bar{\mathbf{I}}\right]^{-1} \bar{\mathbf{z}}^{-}_{N-1,N} \bar{\mathbf{Z}}^{-1}_{(N-1)0}\left[\bar{\mathbf{I}} - \bar{\mathbf{\Gamma}}_{N-1}\right]. \tag{32}$$

Following the steps from (30) to (32) recursively with the form:

$$\bar{\mathbf{Z}}^{-}_{n,n+1} = \bar{\mathbf{I}} + \bar{\mathbf{z}}^{-}_{n,n+1}, \tag{33}$$

$$\bar{\mathbf{z}}^{-}_{n,n+1} = j\beta_0 \bar{\mathbf{O}}_n \left[\sum_{m=n+1}^{N} d_m \bar{\mathbf{O}}^T_m \bar{\mathbf{\Delta}}_m \bar{\mathbf{O}}_m\right] \bar{\mathbf{O}}^T_n. \tag{34}$$

Similar to the approximation to get (32), we have:

$$\bar{\mathbf{R}}^{-}_{n,n+1} \approx \bar{\mathbf{\Gamma}}_n + \left[\bar{\mathbf{Z}}^{-1}_{n0} + \bar{\mathbf{I}}\right]^{-1} \bar{\mathbf{z}}^{-}_{n,n+1} \bar{\mathbf{Z}}^{-1}_{n0}\left[\bar{\mathbf{I}} - \bar{\mathbf{\Gamma}}_n\right], \tag{35}$$

$$\bar{\mathbf{Z}}^{+}_{n-1,n} \approx \bar{\mathbf{I}} + j\beta_0 d_n \bar{\mathbf{\Delta}}_n + \bar{\mathbf{z}}^{-}_{n,n+1} = \bar{\mathbf{I}} + \bar{\mathbf{z}}^{+}_{n-1,n}, \tag{36}$$

where

$$\bar{\mathbf{z}}^{+}_{n-1,n} = j\beta_0 \bar{\mathbf{O}}_n \left[\sum_{m=n}^{N} d_m \bar{\mathbf{O}}^T_m \bar{\mathbf{\Delta}}_m \bar{\mathbf{O}}_m\right] \bar{\mathbf{O}}^T_n. \tag{37}$$

Submitting it to (10), we approximate $\bar{\mathbf{Z}}^{-}_{n-1,n}$ to the form similar to (34). Finally, we have:

$$\bar{\mathbf{Z}}^{-}_{0,1} \approx \bar{\mathbf{I}} + j\beta_0 \sum_{n=1}^{N} d_n \bar{\mathbf{O}}^T_n \bar{\mathbf{\Delta}}_n \bar{\mathbf{O}}_n, \tag{38}$$

and the total reflection coefficient,

$$\bar{\mathbf{R}} = \bar{\mathbf{R}}^{-}_{0,1} \approx \frac{j\beta_0}{2} \sum_{n=1}^{N} d_n \bar{\mathbf{O}}^T_n \bar{\mathbf{\Delta}}_n \bar{\mathbf{O}}_n. \tag{39}$$

The low frequency limit of the total transmission coefficient is found in a similar way as:

$$\bar{\mathbf{T}} \approx \bar{\mathbf{I}} - \frac{j\beta_0}{2} \sum_{n=1}^{N} d_n \bar{\mathbf{O}}^T_n \bar{\mathbf{s}}_n \bar{\mathbf{O}}_n, \tag{40}$$

where $\bar{\mathbf{s}}_n = \mathrm{diag}\left(\mu_{ny} + \varepsilon_{nx}, \mu_{nx} + \varepsilon_{ny}\right)$.

Applying the low frequency limit of the reflection and transmission matrices for equivalent layer and multiple layers to (25) and (26), we have effective parameters as:

$$\begin{aligned} \theta_{et} &= \frac{1}{2}\tan^{-1}\frac{\sum_{n=1}^{N} d_n\left(\varepsilon_{nx} - \varepsilon_{ny} + \mu_{nx} - \mu_{ny}\right)\sin 2\theta_n}{\sum_{n=1}^{N} d_n\left(\varepsilon_{nx} - \varepsilon_{ny} + \mu_{nx} - \mu_{ny}\right)\cos 2\theta_n}, \\ \theta_{er} &= \frac{1}{2}\tan^{-1}\frac{\sum_{n=1}^{N} d_n\left(\varepsilon_{nx} - \varepsilon_{ny} - \mu_{nx} + \mu_{ny}\right)\sin 2\theta_n}{\sum_{n=1}^{N} d_n\left(\varepsilon_{nx} - \varepsilon_{ny} - \mu_{nx} + \mu_{ny}\right)\cos 2\theta_n}, \end{aligned} \tag{41}$$

$$\begin{aligned} \Delta_{xe,ye} &= \frac{1}{2d_t}\sum_{n=1}^{N} d_n\left[\Delta_{nx} + \Delta_{ny} \pm \left(\Delta_{nx} - \Delta_{ny}\right)\frac{\sin 2\theta_n}{\sin 2\theta_{er}}\right], \\ s_{xe,ye} &= \frac{1}{2d_t}\sum_{n=1}^{N} d_n\left[s_{nx} + s_{ny} \pm \left(s_{nx} - s_{ny}\right)\frac{\sin 2\theta_n}{\sin 2\theta_{et}}\right], \end{aligned} \tag{42}$$

where $d_t = \sum_{n=1}^{N} d_n$ and $\boldsymbol{\mu}, \boldsymbol{\varepsilon}$ can be achieved by:

$$\mu_{\tilde{p}e} = \frac{s_{pe} + \Delta_{pe}}{2}, \quad \varepsilon_{pe} = \frac{s_{pe} - \Delta_{pe}}{2}. \tag{43}$$

Here, although there are two kinds of expressions for the effective angle, the relative difference between them is small and is about 1% in difference at frequency up to 10 GHz.

If we consider about non-magnetic materials or $\boldsymbol{\mu}$ is scaler, (41)-(43) can be simplified as:

$$\theta_e = \theta_{er} = \theta_{et} = \frac{1}{2}\tan^{-1}\frac{\sum_{n=1}^{N} d_n\left(\varepsilon_{nx} - \varepsilon_{ny}\right)\sin 2\theta_n}{\sum_{n=1}^{N} d_n\left(\varepsilon_{nx} - \varepsilon_{ny}\right)\cos 2\theta_n}, \tag{44}$$

$$\varepsilon_{xe,ye} = \frac{1}{2d_t}\sum_{n=1}^{N} d_n\left[\varepsilon_{nx} + \varepsilon_{ny} \pm \left(\varepsilon_{nx} - \varepsilon_{ny}\right)\frac{\sin 2\theta_n}{\sin 2\theta_e}\right]. \tag{45}$$

If all layers are same but with different orientations, (41)-(43) can be further simplified as:

$$\theta_e = \theta_{er} = \theta_{et} = \frac{1}{2}\tan^{-1}\frac{\sum_{n=1}^{N} d_n \sin 2\theta_n}{\sum_{n=1}^{N} d_n \cos 2\theta_n}, \tag{46}$$

$$\begin{aligned} \varepsilon_{xe,ye} &= \frac{1}{2}\left[\varepsilon_x + \varepsilon_y \pm \left(\varepsilon_x - \varepsilon_y\right)\frac{\sum_{n=1}^{N} d_n \sin 2\theta_n}{d_t \sin 2\theta_e}\right], \\ \mu_{xe,ye} &= \frac{1}{2}\left[\mu_x + \mu_y \pm \left(\mu_x - \mu_y\right)\frac{\sum_{n=1}^{N} d_n \sin 2\theta_n}{d_t \sin 2\theta_e}\right], \end{aligned} \tag{47}$$

which is the same as the result reported earlier in [7].

The z-component of the effective permittivity and permeability of the multilayered biaxial media can be found [6]:

$$\frac{1}{\varepsilon_{ze}} = \sum_{n=1}^{N}\frac{1}{\varepsilon_{nz}}\frac{d_n}{d_t}, \quad \frac{1}{\mu_{ze}} = \sum_{n=1}^{N}\frac{1}{\mu_{nz}}\frac{d_n}{d_t}. \tag{48}$$

III. NUMERICAL RESULTS

In this section, we present numerical results showing the effective medium theory works well for multilayered anisotropic material with different orientations up to 10 GHz by comparing the parameters extracted without low frequency approximation with the ones with low frequency approximation.

The composite structure investigated is the four-layer non-magnetic medium. Figure 3 plots the real and imaginary parts of relative permittivity and permeability extracted from reflection and transmission coefficients with same thickness, same rotation angles and different relative permittivity (with same loss tangent in four layers) and permeability in x and y directions. Results with and without the low frequency approximation are given. The frequency ranges from 10 MHz to 20 GHz. The real part of relative effective permeability is close to one (the relative permeability with low frequency limit is one in both x and y directions) and has nearly 1% difference at frequency up to 10 GHz. The effective permittivity also works up to 10 GHz. At low frequency range, the imaginary part of relative permeability is zero and imaginary part of relative permittivity is negative due to loss. When the frequency goes up, the relative permittivity and permeability would have imaginary parts with opposite signs, but the attenuation constant is still positive [11].

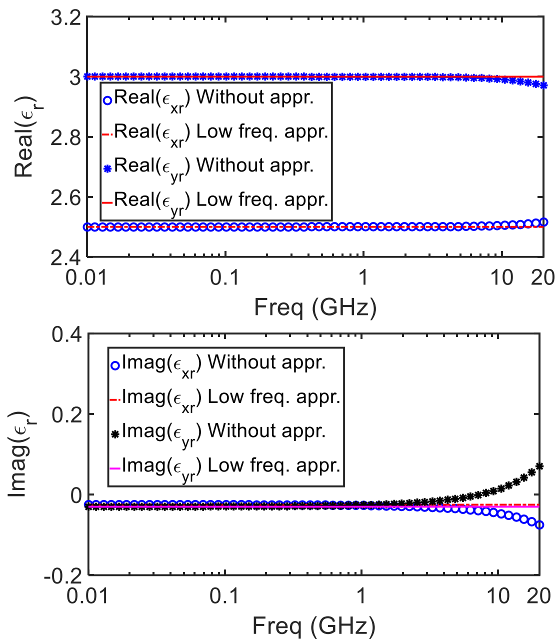

(a) Relative permittivity in x and y directions

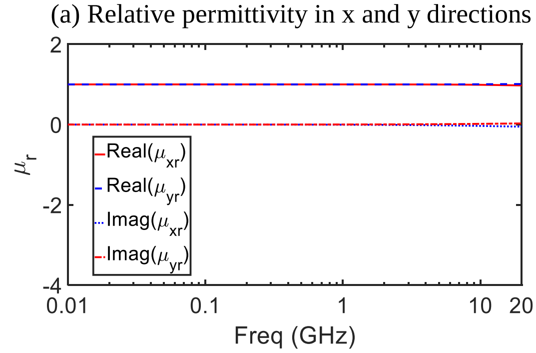

(b) Relative permeability in *x* and *y* directions

Fig. 3. Real and imaginary parts of relative permittivity and permeability of equivalent model with and without low frequency approximation for 4-layer biaxial non-magnetic media. $d_{1,2,3,4} = 0.375$ mm, $\varepsilon_{x2,x4} = 3(1-0.01j)$, $\varepsilon_{y1,y3} = 4(1-0.01j)$, $\varepsilon_{x1,x3,y2,y4} = 2(1-0.01j)$, $\theta_{1,2,3,4} = 30°$, $\theta_e = 30°$.

Figure 4 plots the real part of relative permittivity and permeability extracted from reflection and transmission coefficients with same thickness, different rotation angles and different relative permittivity and permeability in *x* and *y* directions. Again, there is a very good agreement for relative dielectric constants and effective angle between low frequency approximation and without it. The real part of relative effective permeability is almost one for frequency up to several GHz. Comparing without low frequency approximation the frequency independent model has a good agreement for frequency up to 10 GHz.

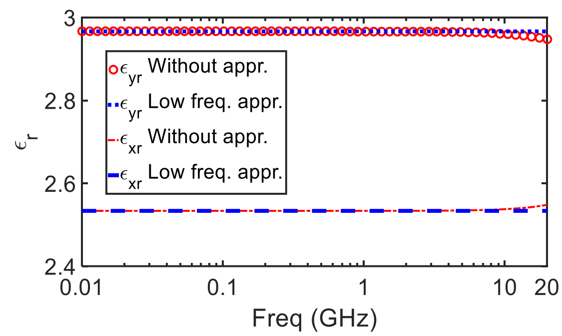

(a) Relative permittivity in x and y directions

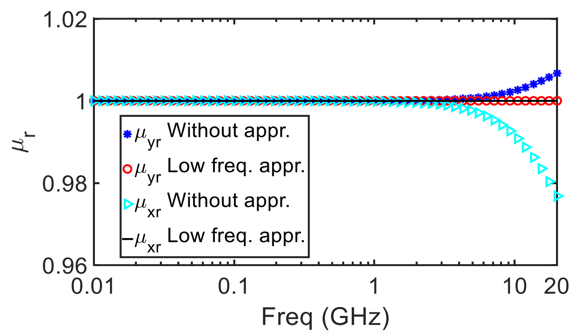

(b) Relative permeability in x and y directions

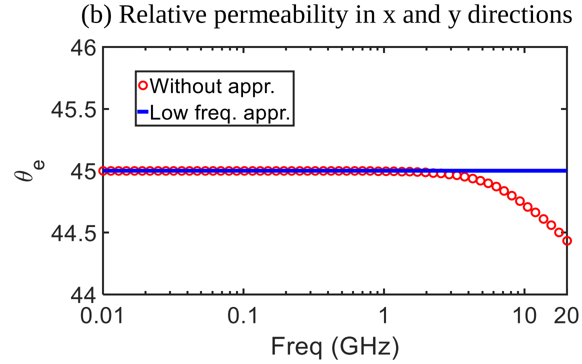

(c) Effective angle

Fig. 4. Real part of relative permittivity and permeability of equivalent model with and without low frequency approximation for different 4-layer biaxial non-magnetic media. $d_{1,2,3,4} = 0.375$ mm, $\theta_{1,4} = 30°$, $\theta_{2,3} = 60°$, $\varepsilon_{x2,x4} = 3$, $\varepsilon_{y1,y3} = 4$, $\varepsilon_{x1,x3,y2,y4} = 2$.

IV. CONCLUSION

We have presented the method to model the multilayered biaxial anisotropic material with different orientation using effective medium theory. By using this method, multilayered biaxial anisotropic media with different orientations can be numerically regarded as an effective medium. A frequency independent model is derived using the low frequency approximation. Numerical examples show the good agreements for effective parameters between with and without low frequency approximation for the frequency up to 10 GHz.

ACKNOWLEDGMENT

This work is supported in part by the NSF IUCRC Program of the Center for Nondestructive Evaluation at Iowa State University and by the China Scholarship Council.

REFERENCES

[1] L. A. Pilato and M. J. Michno, *Advanced Composite Materials*. Springer-Verlag, 1994.

[2] H. M. Flower, *High Performance Materials in Aerospace*. Chapman & Hall, 1995.

[3] H.-C. Chu, S.-K. Jeng, and C.-H. Chen, "Reflection and transmission characteristics of lossy periodic composite structures," *IEEE Trans. Antennas Propag*., vol. 44, no. 3, pp. 580-587, Mar. 1996.

[4] C. L. Holloway, M. S. Sarto, and M. Johansson, "Analyzing carbon-fiber composite materials with equivalent-layer models," *IEEE Trans. Electromagn. Compat*., vol. 47, no. 4, pp. 368-381, Aug. 2001.

[5] M. S. Sarto, S. Di Michele, and P. Leerkamp, "Electromagnetic performance of innovative lightweight shields to reduce radiated emissions from PCBs," *IEEE Trans. Electromagn. Compat*., vol. 44, no. 2, pp. 353-363, May 2002.

[6] F. G. Hu, J. M. Song, and T. Kamgaing, "Modeling of multilayered media using effective medium theory," *IEEE Electrical Performance of Electronic Packaging and Systems*, pp. 225-228, Oct. 2010.

[7] Y. Bao and J. M. Song, "Modeling of multilayered anisotropic media using effective medium theory," *IEEE Antennas and Propagation International Symposium*, Paper WEP-A4. 2P. 2, pp. 2097-2098, Fajardo, PR, June 2016.

[8] W. C. Chew, *Waves and Fields in Inhomogeneous Media*. IEEE Press, pp. 133-140, 1995.

[9] D. R. Smith, S. Schultz, P. Marko, and C. M. Soukoulis, "Determination of effective permittivity and permeability of metamaterials from reflection and transmission coefficients," *Phys. Rev. B*, vol. 65, 195104, Apr. 2002.

[10] X. D. Chen, T. M. Grzegorczyk, B. I. Wu, J. Pacheco, and J. A. Kong, "Robust method to retrieve the constitutive effective parameters of metamaterials," *Phys. Rev. E*, vol. 70, 016608, 2004.

[11] J. Wang, T. Zhao, J. Song, and K. Telesphor, "Modeling of multilayered media for oblique incidence using effective medium theory," *Annual Review of Progress in Applied Computational Electromagnetics*, Columbus, OH, pp. 812-817, Apr. 2012.

[12] S. Arslanagic, T. V. Hansen, N. A. Mortensen, A. H. Gregersen, O. Sigmund, R. W. Ziolkowski, and O. Breinbjerg, "A review of the scattering-parameter extraction method with clarification of ambiguity issues in relation to metamaterial homogenization," *IEEE Antennas Propag. Mag*., vol. 55, no. 2, pp. 91-106, Apr. 2013.

[13] T. Zhao, J. Song, and T. Kamgaing, "IE based approach to determine the effective constitutive parameters of periodic structure using microstrip measurement," *2016 IEEE International Workshop on Electromagnetics: Applications and Student Innovation Competition (iWEM)*, Nanjing, China, pp. 1-3, May 2016.

Yang Bao was born in Nanjing, Jiangsu, China. He received the B.S. and M.S. degrees in Nanjing University of Posts and Telecommunications in 2011 and 2014, respectively. He is currently working toward his Ph.D. in Department of Electrical and Computer Engineering in Iowa State University. His research interests focus on modeling and simulations of composite material, electromagnetic wave scattering using fast algorithms and eddy current nondestructive evaluation.

Jiming Song received the B.S. and M.S. degrees in Physics from Nanjing University, China, in 1983 and 1988, respectively, and the Ph.D. degree in Electrical Engineering from Michigan State University, East Lansing, in 1993.

From 1993 to 2000, he worked as a Postdoctoral Research Associate, a Research Scientist and Visiting Assistant Professor at the University of Illinois at Urbana-Champaign. From 1996 to 2000, he worked part-time as a Research Scientist at SAIC-DEMACO. Song was the principal author of the Fast Illinois Solver Code (FISC). He was a Principal Staff Engineer/Scientist at Semiconductor Products Sector of Motorola in Tempe, Arizona before he joined Department of Electrical and Computer Engineering at Iowa State University as an Assistant Professor in 2002.

Song currently is a Professor at Iowa State University's Department of Electrical and Computer Engineering. His research has dealt with modeling and simulations of interconnects on lossy silicon and RF components, electromagnetic wave scattering using fast algorithms, the wave propagation in metamaterials, acoustic and elastic wave propagation and non-destructive evaluation, and transient electromagnetic field. He was selected as a National Research Council/ Air Force Summer Faculty Fellow in 2004 and 2005 and received the NSF Career Award in 2006. Song is an IEEE Fellow, an Associate Editor for *IEEE Antennas and Wireless Propagation Letters* (AWPL) and *ACES Express*.